

SUPPORTING INFORMATION

ENHANCED PROPERTIES OF A BENZIMIDAZOLE BENZYLPIRAZOLE LYSINE DEMETHYLASE INHIBITOR: MECHANISM-OF-ACTION, BINDING SITE ANALYSIS AND ACTIVITY IN CELLULAR MODELS OF PROSTATE CANCER

David M. Carter¹, Edgar Specker², Piotr H. Małecki^{1,3,4}, Jessica Przygodda², Krystyna Dudaniec¹, Manfred S. Weiss³, Udo Heinemann^{1*}, Marc Nazaré^{2*}, Ulrich Gohlke¹

¹ Max Delbrück Center for Molecular Medicine in the Helmholtz Gemeinschaft (MDC), Berlin, 13125 Germany

² Leibniz-Forschungsinstitut für Molekulare Pharmakologie (FMP), Berlin, 13125 Germany

³ Helmholtz-Zentrum Berlin (HZB) Macromolecular Crystallography, Berlin, 14109 Germany

⁴ Laboratory of Structural Microbiology, Institute of Bioorganic Chemistry, Polish Academy of Sciences, Poznan, 61-704 Poland

Corresponding Authors

*E-mail: heinemann@mdc-berlin.de. Phone: (+49) 30 9406-3420. Fax: (+49) 30 9406-2548.

*E-mail: nazare@fmp-berlin.de. Phone: (+49) 30 9406-3083. Fax: (+49) 30 9406-3084.

CONTENTS OF SUPPORTING INFORMATION:

Molecular Formula Strings

HPLC chromatograms of lead compounds 2, 7, 11, 15, 26, 29, and 30

Table S1. Synthetic Derivatives of a Benzimidazole Pyrazole-based JmjC-KDM Inhibitor

Table S2. Crystallographic Data

Figure S1. Inhibitory properties of selected KDM4 inhibitors, designed to assess H-bonding capacity within the KDM4E active site.

Figure S2. Inhibitory properties of selected KDM4 inhibitors, designed to assess substituted amine binding within the KDM4E active site.

Figure S3. Inhibitory properties of selected KDM4 inhibitors, designed to assess inhibitor sidechain polarity at the R2 scaffold position.

Figure S4. Inhibitory properties of selected KDM4 inhibitors, designed to further assess inhibitor sidechain polarity at R1 and R2 scaffold positions.

Figure S5. Inhibitory properties of focused KDM4 inhibitors, designed or selected to characterize substitutions of the pyrazole hydroxyl moiety.

Figure S6. Inhibitory properties of selected KDM4 inhibitors, designed to assess the potential of active site Fe²⁺ chelation via the scaffold's bidentate chelation motif.

Figure S7. Inhibitory properties of selected KDM4 inhibitors, designed to assess the contribution of the scaffold's benzimidazole function towards inhibitory efficacy.

Figure S8. Inhibitory properties of selected KDM4 inhibitors, designed to assess the possibility to derivatize the scaffold's benzimidazole function.

Figure S9. Enhanced properties of a benzimidazole benzylpyrazole KDM4E inhibitor do not affect activity of the coupling enzyme, formaldehyde dehydrogenase.

Figure S10. Compound 15 is active in cellular models of prostate cancer.

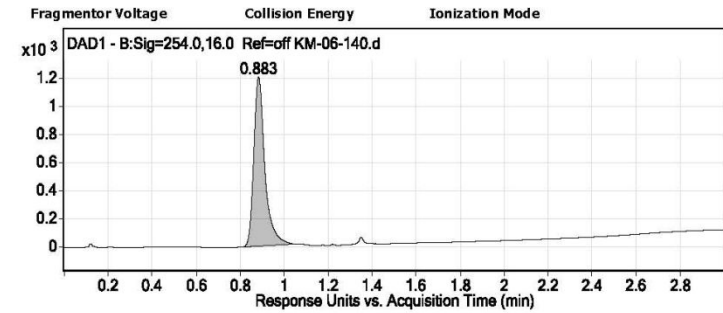
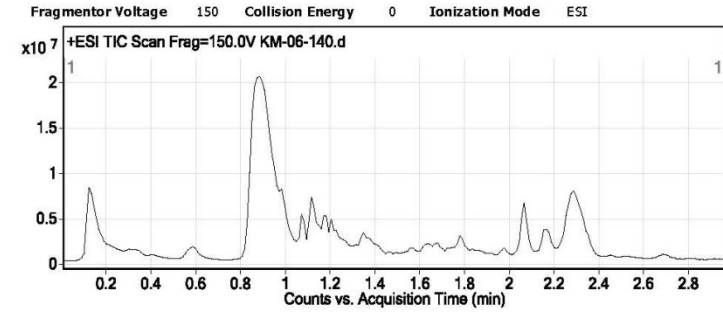
Molecular Formula Strings

Compound	Smiles	IC ₅₀ (μM)
1	<chem>OC1=CC(CC(OC)=O)=NN1C2=NC3=CC=CC=C3N2</chem>	15
1	<chem>OC1=CC(CC(OC)=O)=NN1C2=NC3=CC=CC=C3N2</chem>	581
2	<chem>OC1=CC(CC(O)=O)=NN1C2=NC3=CC=CC=C3N2</chem>	34
3	<chem>OC1=C(CCC(OC)=O)C(C)=NN1C2=NC3=CC=CC=C3N2</chem>	72
4	<chem>OC1=C(C)C(CCC(OC)=O)=NN1C2=NC3=CC=CC=C3N2</chem>	106
5	<chem>OC1=C(CCC(O)=O)C(C)=NN1C2=NC3=CC=CC=C3N2</chem>	274
6	<chem>OC1=C(C)C(CCC(O)=O)=NN1C2=NC3=CC=CC=C3N2</chem>	437
7	<chem>OC1=C(CCC(NC)=O)C(C)=NN1C2=NC3=CC=CC=C3N2</chem>	41
8	<chem>OC1=C(CCC(N(C)C)=O)C(C)=NN1C2=NC3=CC=CC=C3N2</chem>	16
9	<chem>OC1=C(CCCNC)C(C)=NN1C2=NC3=CC=CC=C3N2</chem>	9
10	<chem>OC1=C(CCCN(C)C)C(C)=NN1C2=NC3=CC=CC=C3N2</chem>	70
11	<chem>OC1=CC(C)=NN1C2=NC3=CC=CC=C3N2</chem>	76
12	<chem>OC1=C(CC=C)C(C)=NN1C2=NC3=CC=CC=C3N2</chem>	24
13	<chem>OC1=C(CCC)C(C)=NN1C2=NC3=CC=CC=C3N2</chem>	24
14	<chem>OC1=C(CC#C)C(C)=NN1C2=NC3=CC=CC=C3N2</chem>	5
15	<chem>OC1=C(C2=CC=CC=C2)C(C)=NN1C3=NC4=CC=CC=C4N3</chem>	0.9
15	<chem>OC1=C(C2=CC=CC=C2)C(C)=NN1C3=NC4=CC=CC=C4N3</chem>	13
16	<chem>OC1=C(CC2=CC=CC=C2)C(C)=NN1C3=NC4=CC=CC=C4N3</chem>	27
17	<chem>OC1=C(C2=CC=C(C)C=C2)C(C)=NN1C3=NC4=CC=CC=C4N3</chem>	27
18	<chem>OC1=C(C2=CC=CC=C2)C(CC)=NN1C3=NC4=CC=CC=C4N3</chem>	5
19	<chem>OC1=C(C2=CC=CC=C2)C(CCCC)=NN1C3=NC4=CC=CC=C4N3</chem>	6
20	<chem>OC1=C(Br)C=NN1C2=NC3=CC=CC=C3N2</chem>	NI*
21	<chem>CC1=CC(C)=NN1C2=NC3=CC=CC=C3N2</chem>	NI
22	<chem>NC1=CC(C)=NN1C2=NC3=CC=CC=C3N2</chem>	199
23	<chem>NC1=C(C2=CC=CC=C2)C(C)=NN1C3=NC4=CC=CC=C4N3</chem>	~160
24	<chem>OC1=C(C2=CC=CC=C2)C(C)=NN1C3=NC4=CC=CC=C4S3</chem>	35
25	<chem>OC1=C(C2=CC=CC=C2)C(C)=NN1C3=NC4=CC=CC=C4N3C</chem>	34
26	<chem>OC1=C(C2=CC=CC=C2)C(C)=NN1C3=NC=CC=C3</chem>	74
27	<chem>OC1=C(CC2=CC=CC=C2)C(C)=NN1C3=NC=CC=C3</chem>	57
28	<chem>OC1=C(CC=C)C(C)=NN1C2=NC=CC=C2</chem>	191
29	<chem>OC1=C(C2=CC=CC=C2)C(C)=NN1C3=NN=C(Cl)C=C3</chem>	68
30	<chem>OC1=C(C2=CC=CC=C2)C(C)=NN1C3=NC4=C(C=C(C(O)=O)C=C4)N3</chem>	19

*No Inhibition

QC data: Compound 2

Qualitative Compound Report



User Chromatogram Peak List

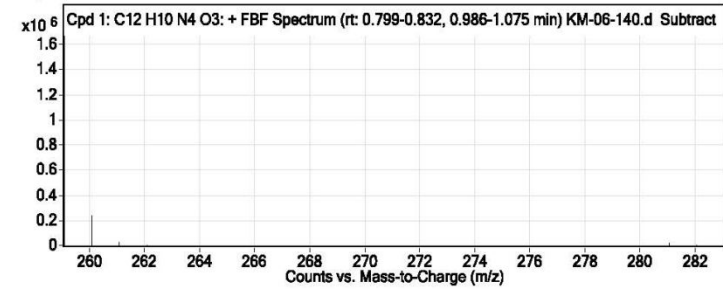
Compound Name	Compound Number	RT	Height	Height %	Area	Area %	Area Sum %	Width
Cpd 1: 0.887	1	0.883	1204.16	100	4224.62	100	100	0.247

Compound Table

Compound Label	RT	Mass	Abund	Formula	Tgt Mass	Diff (ppm)	Purity Value	Purity Result
Cpd 1: C12 H10 N4 O3	0.887	258.0757	17284	C12 H10 N4 O3	258.0753	1.46	100	Pass

Compound Label	m/z	RT	Algorithm	Mass
Cpd 1: C12 H10 N4 O3	281.0648	0.887	Find By Formula	258.0757

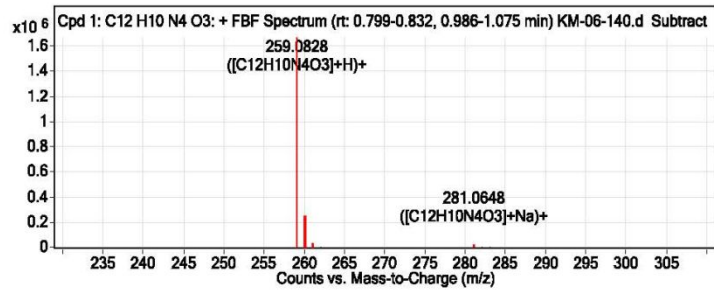
MS Spectrum



MS Zoomed Spectrum

QC Data: Compound 2 continued.

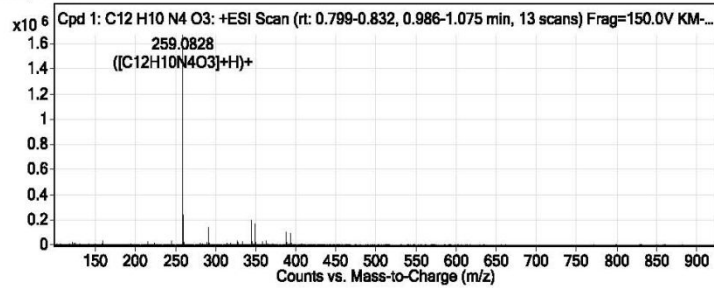
Qualitative Compound Report



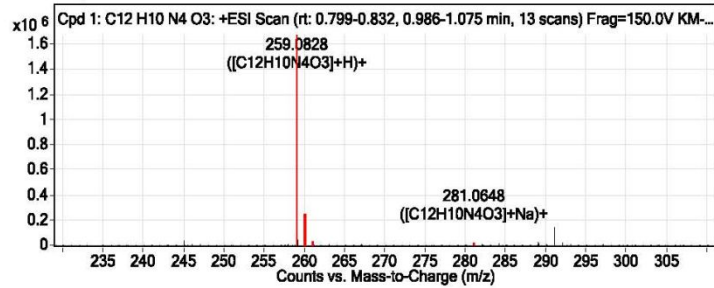
MS Spectrum Peak List

m/z	z	Abund	Formula	Ion
259.0828	1	1669480.75	C12H10N4O3	(M+H)+
260.0865	1	235708.14	C12H10N4O3	(M+H)+
261.0885	1	21914.65	C12H10N4O3	(M+H)+
262.0913	1	1777.77	C12H10N4O3	(M+H)+
281.0648	1	17284.46	C12H10N4O3	(M+Na)+
282.0675	1	2443.94	C12H10N4O3	(M+Na)+
283.072	1	204.28	C12H10N4O3	(M+Na)+

MS Spectrum



MS Zoomed Spectrum



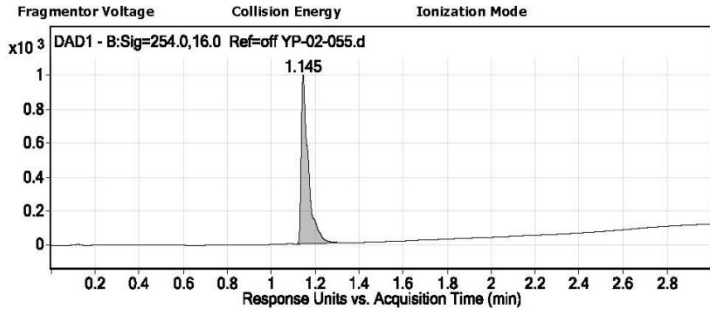
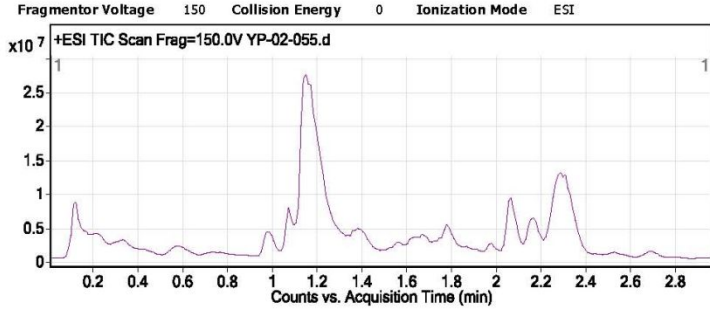
MS Spectrum Peak List

m/z	Calc m/z	Diff(ppm)	z	Abund	Formula	Ion
259.0828	259.0826	-1	1	1669480.75	C12H10N4O3	(M+H)+
260.0865	260.0853	-4.47	1	235708.14	C12H10N4O3	(M+H)+
261.0885	261.0876	-3.69	1	21914.65	C12H10N4O3	(M+H)+
262.0913	262.0899	-5.24	1	1777.77	C12H10N4O3	(M+H)+
281.0648	281.0645	-0.92	1	17284.46	C12H10N4O3	(M+Na)+
282.0675	282.0673	-0.89	1	2443.94	C12H10N4O3	(M+Na)+
283.072	283.0695	-8.89	1	204.28	C12H10N4O3	(M+Na)+

--- End Of Report ---

QC Data: Compound 7

Qualitative Compound Report



User Chromatogram Peak List

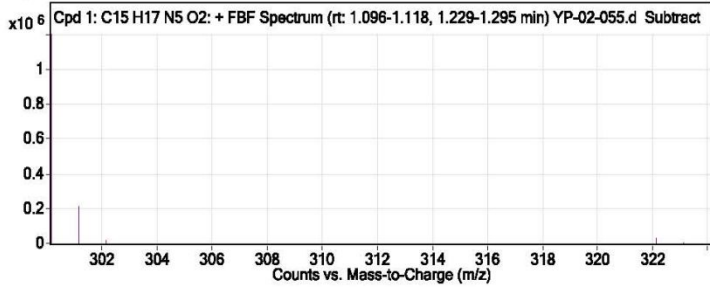
Compound Name	Compound Number	RT	Height	Height %	Area	Area %	Area Sum %	Width
Cpd 1: 1.162	1	1.145	994.37	100	2249.11	100	100	0.22

Compound Table

Compound Label	RT	Mass	Abund	Formula	Tgt Mass	Diff (ppm)	Purity Value	Purity Result
Cpd 1: C15 H17 N5 O2	1.162	299.1383	1205334	C15 H17 N5 O2	299.1382	0.29	100	Pass

Compound Label	m/z	RT	Algorithm	Mass
Cpd 1: C15 H17 N5 O2	300.1455	1.162	Find By Formula	299.1383

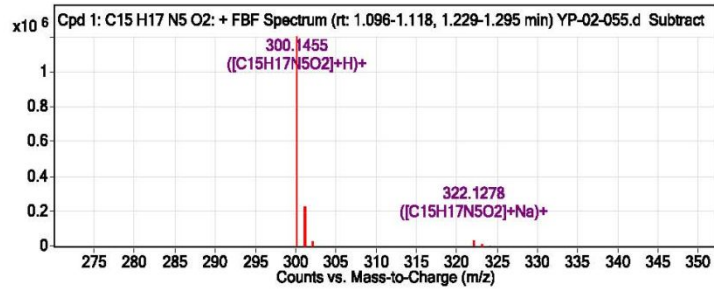
MS Spectrum



MS Zoomed Spectrum

QC Data: Compound 7 Continued.

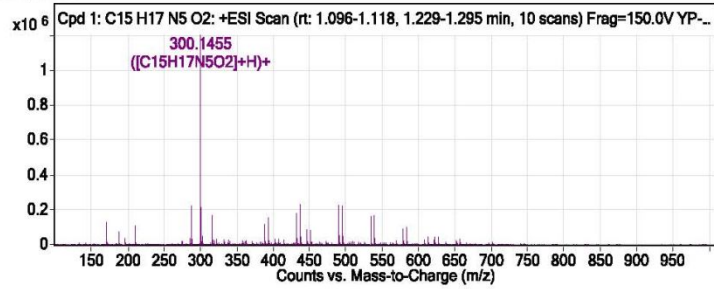
Qualitative Compound Report



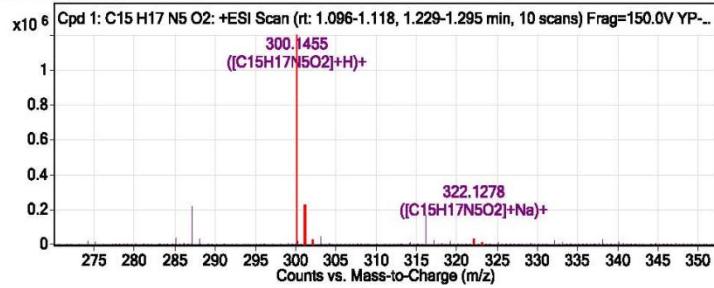
MS Spectrum Peak List

m/z	z	Abund	Formula	Ion
300.1455	1	1205334.38	C15H17N5O2	(M+H)+
301.1487	1	211612.83	C15H17N5O2	(M+H)+
302.1512	1	18919.61	C15H17N5O2	(M+H)+
322.1278	1	32007.41	C15H17N5O2	(M+Na)+
323.1309	1	5530.36	C15H17N5O2	(M+Na)+
324.1371	1	749.17	C15H17N5O2	(M+Na)+

MS Spectrum



MS Zoomed Spectrum



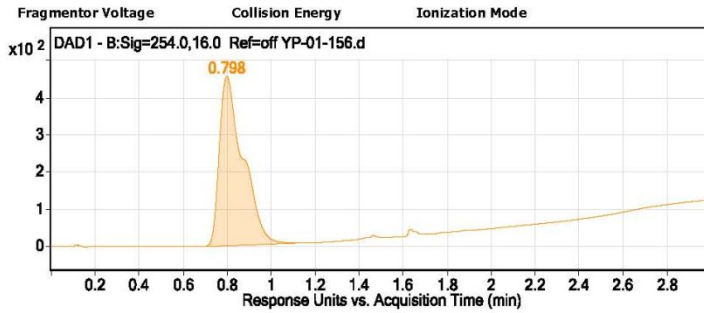
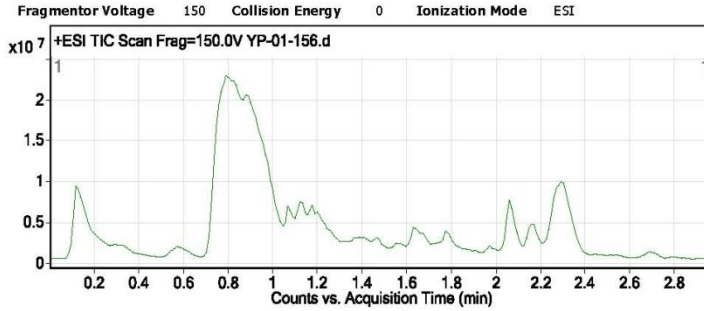
MS Spectrum Peak List

m/z	Calc m/z	Diff(ppm)	z	Abund	Formula	Ion
300.1455	300.1455	0	1	1205334.38	C15H17N5O2	(M+H)+
301.1487	301.1483	-1.58	1	211612.83	C15H17N5O2	(M+H)+
302.1512	302.1507	-1.42	1	18919.61	C15H17N5O2	(M+H)+
322.1278	322.1274	-1.11	1	32007.41	C15H17N5O2	(M+Na)+
323.1309	323.1302	-2.3	1	5530.36	C15H17N5O2	(M+Na)+
324.1371	324.1327	-13.66	1	749.17	C15H17N5O2	(M+Na)+

--- End Of Report ---

QC Data: Compound 11

Qualitative Compound Report



User Chromatogram Peak List

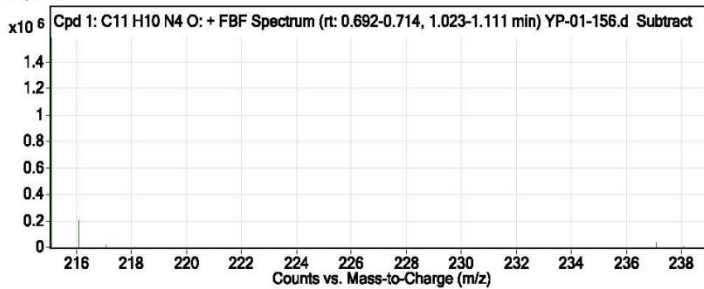
Compound Name	Compound Number	RT	Height	Height %	Area	Area %	Area Sum %	Width
Cpd 1: 0.813	1	0.798	457.28	100	3409.5	100	100	0.443

Compound Table

Compound Label	RT	Mass	Abund	Formula	Tgt Mass	Diff (ppm)	Purity Value	Purity Result
Cpd 1: C11 H10 N4 O	0.813	214.0855	36453	C11 H10 N4 O	214.0855	0.21	100	Pass

Compound Label	m/z	RT	Algorithm	Mass
Cpd 1: C11 H10 N4 O	237.075	0.813	Find By Formula	214.0855

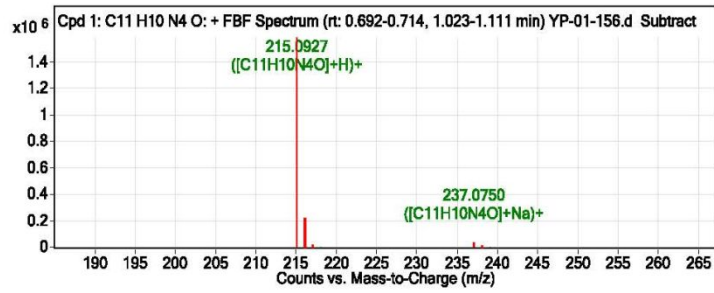
MS Spectrum



MS Zoomed Spectrum

QC Data: Compound 11 continued.

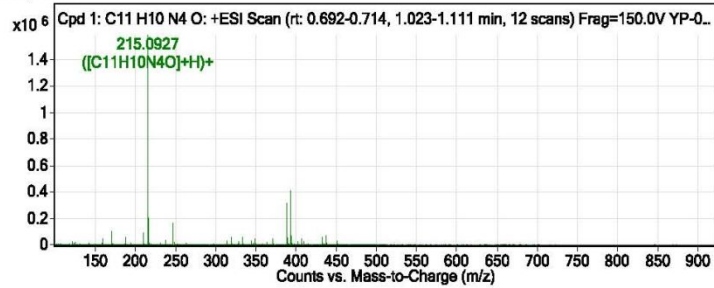
Qualitative Compound Report



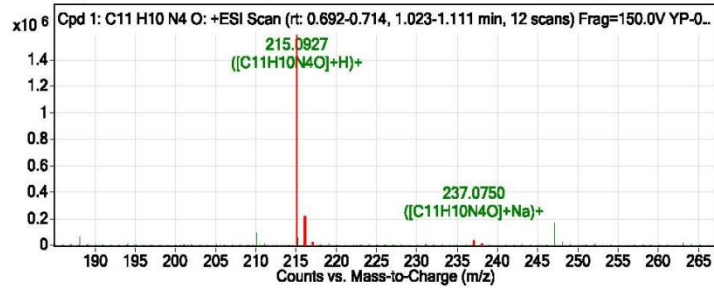
MS Spectrum Peak List

m/z	z	Abund	Formula	Ion
215.0927	1	1583945.63	C11H10N4O	(M+H)+
216.0961	1	203982.45	C11H10N4O	(M+H)+
217.099	1	15169.42	C11H10N4O	(M+H)+
218.0997	1	1053.96	C11H10N4O	(M+H)+
237.075	1	36453.02	C11H10N4O	(M+Na)+
238.0776	1	4451.94	C11H10N4O	(M+Na)+
239.084	1	375.8	C11H10N4O	(M+Na)+

MS Spectrum



MS Zoomed Spectrum

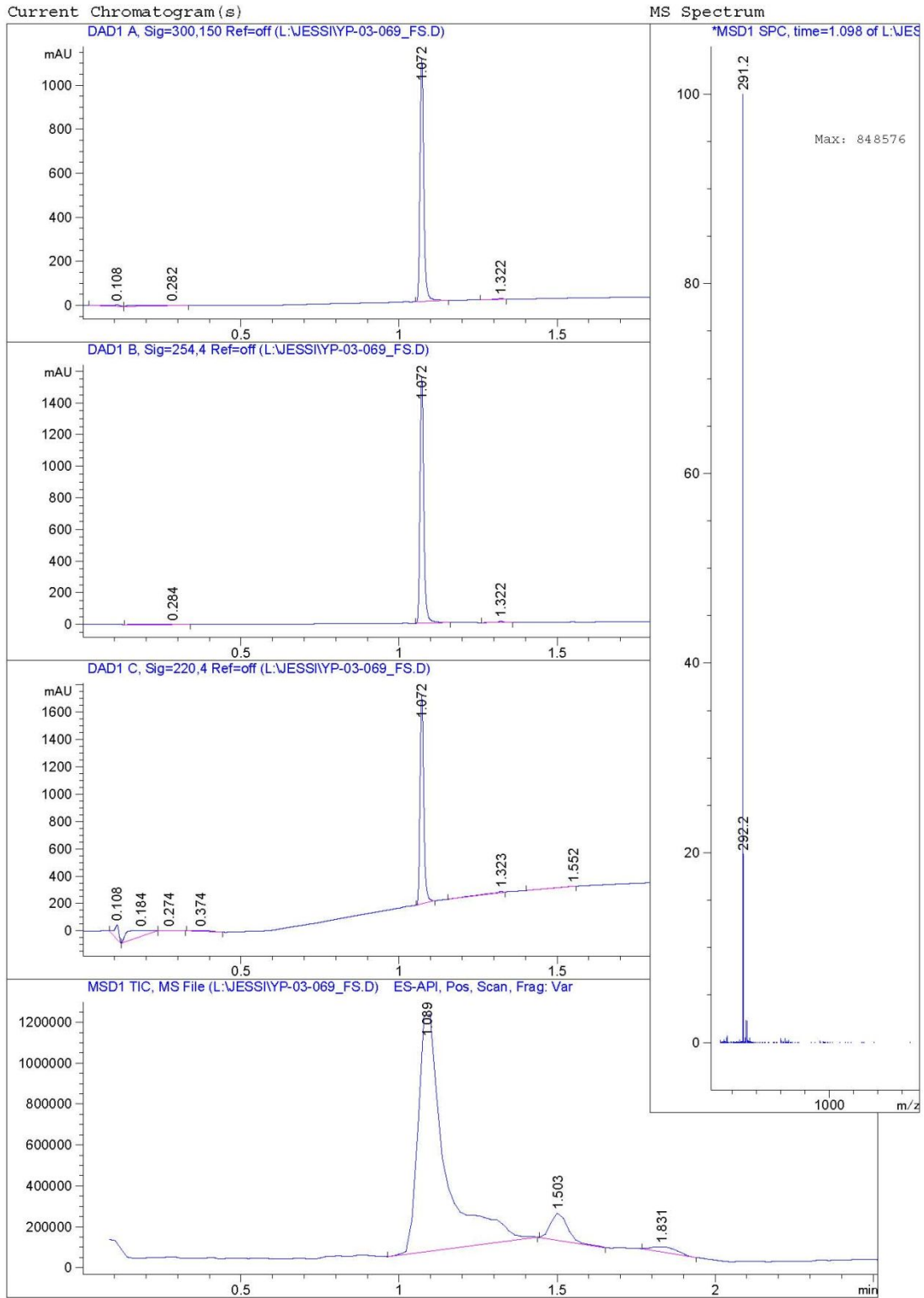


MS Spectrum Peak List

m/z	Calc m/z	Diff(ppm)	z	Abund	Formula	Ion
215.0927	215.0927	0.26	1	1583945.63	C11H10N4O	(M+H)+
216.0961	216.0954	-3.24	1	203982.45	C11H10N4O	(M+H)+
217.099	217.0979	-5.45	1	15169.42	C11H10N4O	(M+H)+
218.0997	218.1002	2.23	1	1053.96	C11H10N4O	(M+H)+
237.075	237.0747	-1.26	1	36453.02	C11H10N4O	(M+Na)+
238.0776	238.0774	-0.96	1	4451.94	C11H10N4O	(M+Na)+
239.084	239.0798	-17.74	1	375.8	C11H10N4O	(M+Na)+

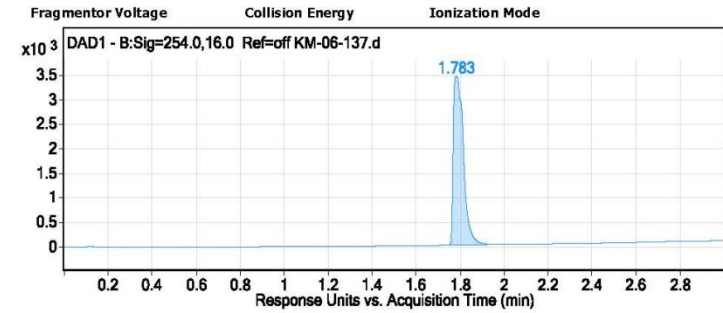
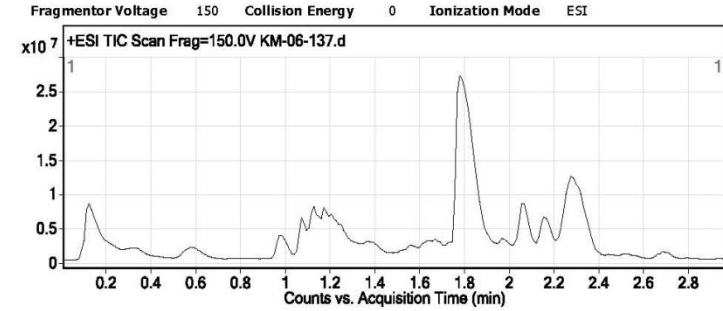
--- End Of Report ---

QC Data: Compound 15



QC Data: Compound 26

Qualitative Compound Report



User Chromatogram Peak List

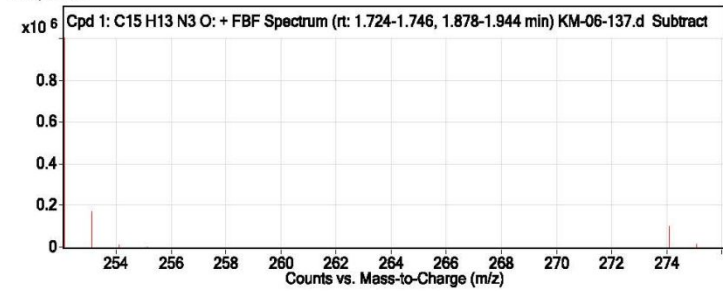
Compound Name	Compound Number	RT	Height	Height %	Area	Area %	Area Sum %	Width
Cpd 1: 1.801	1	1.783	3446.2	100	11072.13	100	100	0.278

Compound Table

Compound Label	RT	Mass	Abund	Formula	Tgt Mass	Diff (ppm)	Purity Value	Purity Result
Cpd 1: C15 H13 N3 O	1.801	251.1065	1005455	C15 H13 N3 O	251.1059	2.66	100	Pass

Compound Label	m/z	RT	Algorithm	Mass
Cpd 1: C15 H13 N3 O	252.1137	1.801	Find By Formula	251.1065

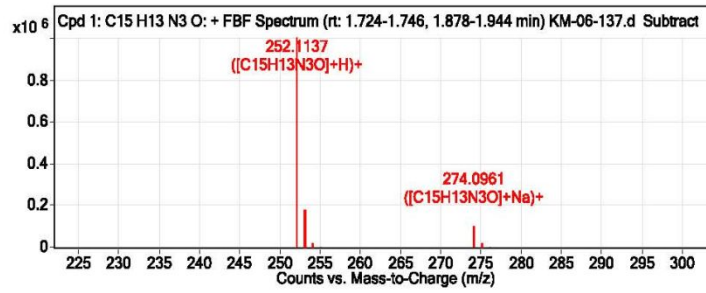
MS Spectrum



MS Zoomed Spectrum

QC Data: Compound 26 continued.

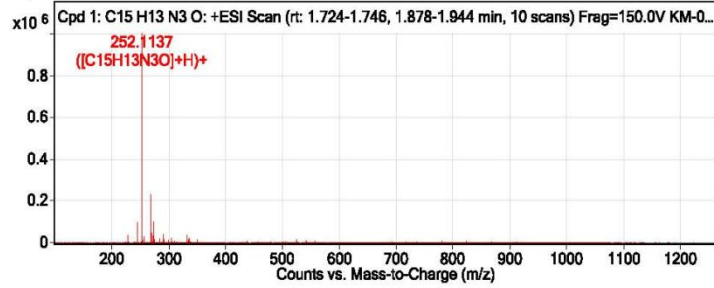
Qualitative Compound Report



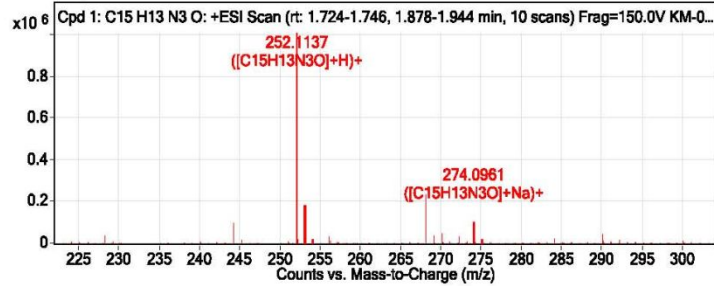
MS Spectrum Peak List

m/z	z	Abund	Formula	Ion
252.1137	1	1005454.63	C15H13N3O	(M+H)+
253.1173	1	169138.77	C15H13N3O	(M+H)+
254.1199	1	12746.42	C15H13N3O	(M+H)+
255.1221	1	934.2	C15H13N3O	(M+H)+
274.0961	1	100997.13	C15H13N3O	(M+Na)+
275.0989	1	14722.76	C15H13N3O	(M+Na)+
276.1013	1	1340.76	C15H13N3O	(M+Na)+

MS Spectrum



MS Zoomed Spectrum



MS Spectrum Peak List

m/z	Calc m/z	Diff(ppm)	z	Abund	Formula	Ion
252.1137	252.1131	-2.11	1	1005454.63	C15H13N3O	(M+H)+
253.1173	253.1161	-4.82	1	169138.77	C15H13N3O	(M+H)+
254.1199	254.1169	-3.99	1	12746.42	C15H13N3O	(M+H)+
255.1221	255.1215	-2.26	1	934.2	C15H13N3O	(M+H)+
274.0961	274.0951	-3.85	1	100997.13	C15H13N3O	(M+Na)+
275.0989	275.0981	-2.87	1	14722.76	C15H13N3O	(M+Na)+
276.1013	276.1008	-1.59	1	1340.76	C15H13N3O	(M+Na)+

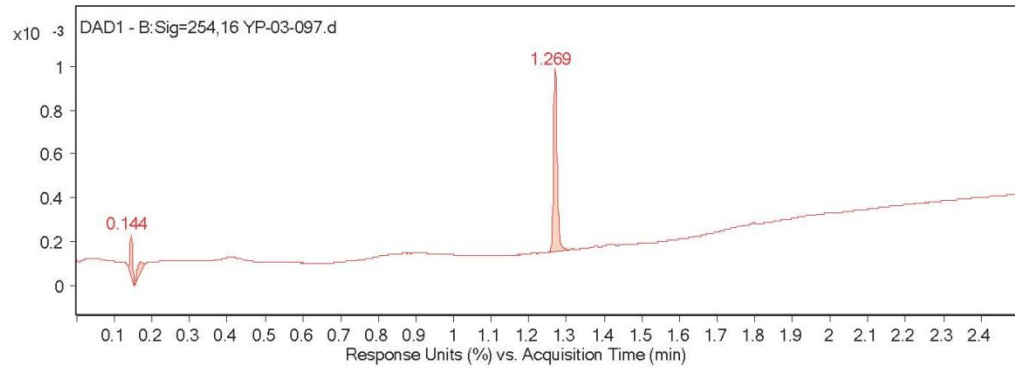
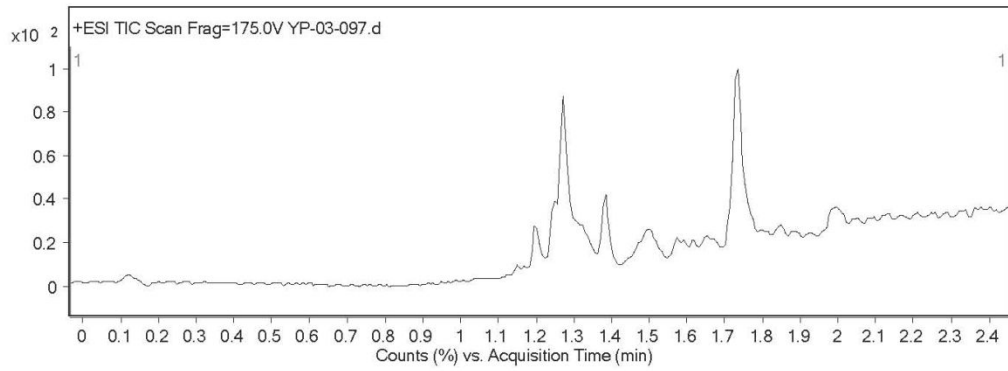
--- End Of Report ---

QC Data: Compound 29

Qualitative Analysis Report

User Chromatograms

Fragmentor Voltage 175 Collision Energy 0 Ionization Mode ESI

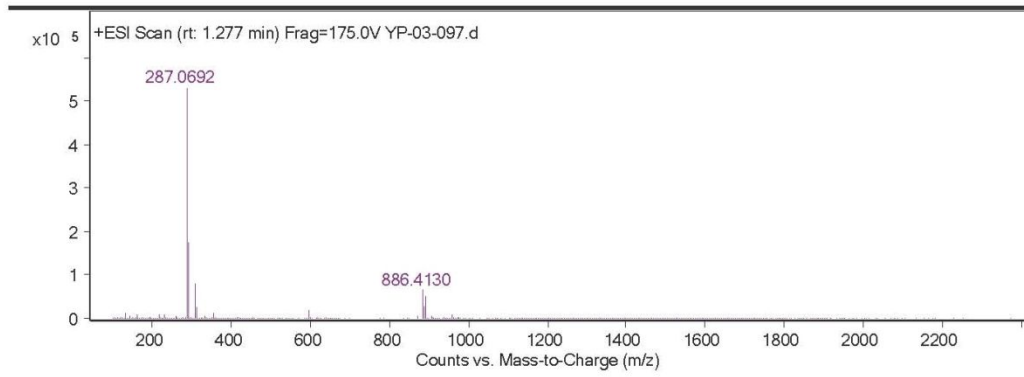


User Spectra

Fragmentor Voltage	Collision Energy	Ionization Mode
175	0	ESI

QC Data: Compound 29 continued.

Qualitative Analysis Report



--- End Of Report ---

QC Data: Compound 30

Current Chromatogram(s)

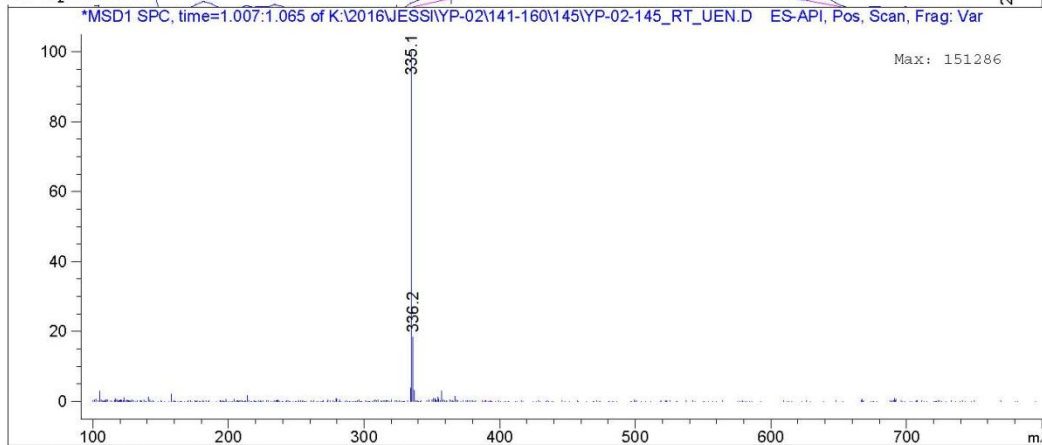
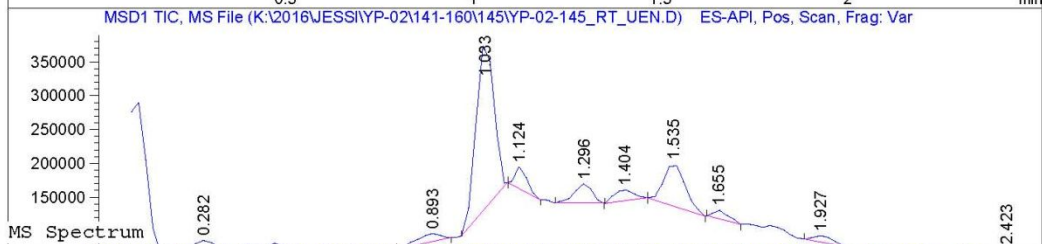
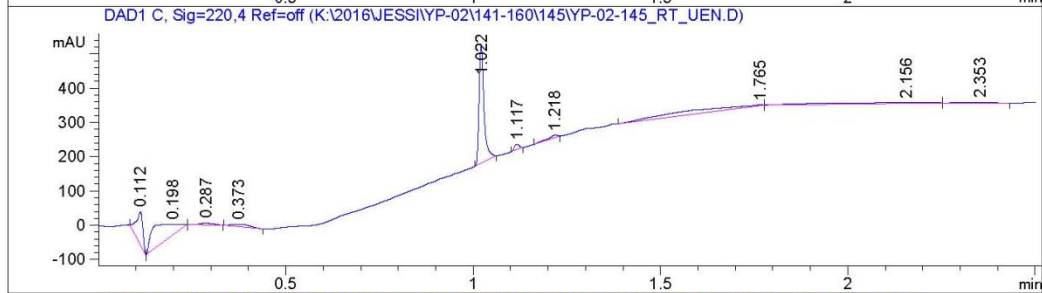
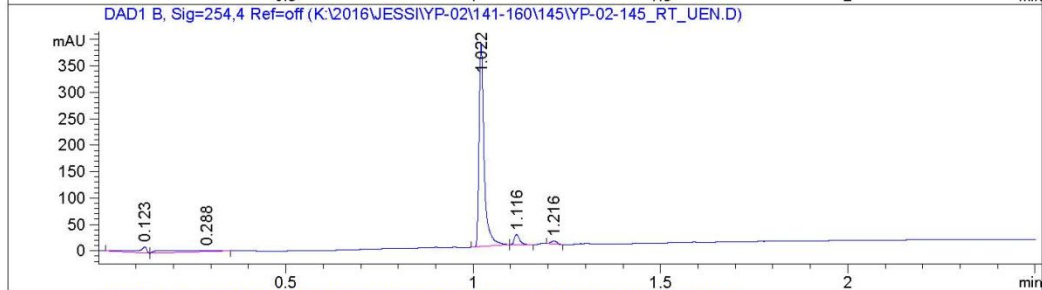
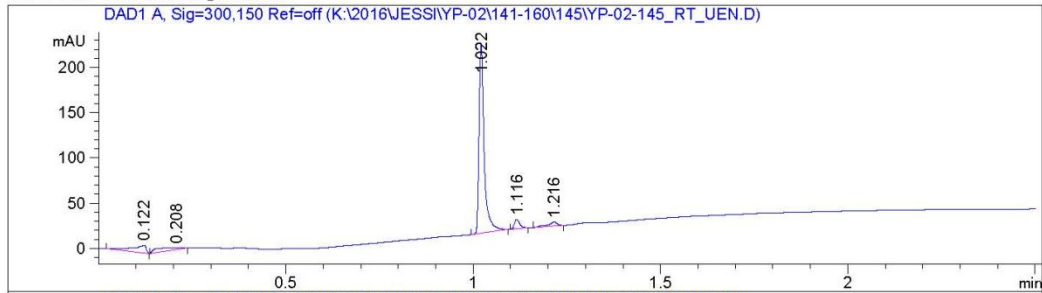
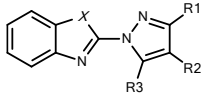
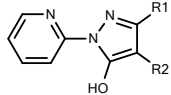
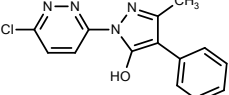
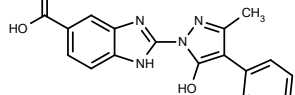


Table S1. Synthetic Derivatives of a Benzimidazole Pyrazole-based JmjC-KDM Inhibitor

Benzimidazole pyrazoles		Pyridine pyrazoles		Pyridazine-substituted Variant		Carboxy-substituted Variant				
										
cmpds 1-25		cmpds 26-28		cmpd 29		cmpd 30				
Benzimidazole pyrazole-based scaffold					Best Fit Parameters					
cmpd	X	R1	R2	R3	IC ₅₀ μM ^a	IC ₅₀ 95% CI μM ^b	top ^c	bottom ^d	Hill slope ^e	residual ^f
1 ^g	NH	CH ₂ CO ₂ Me	H	OH	15	12–19	105%	2%	-1.1	2%
1 ^h	NH	CH ₂ CO ₂ Me	H	OH	581 ⁱ	486–696	100%	0%	0.8	10%
2	NH	CH ₂ CO ₂ H	H	OH	347	293–411	96%	-5%	-1.6	1%
3	NH	Me	CH ₂ CH ₂ CO ₂ Me	OH	72	68–77	96%	0%	-2.3	1%
4	NH	CH ₂ CH ₂ CO ₂ Me	Me	OH	106	97–117	101%	2%	-2.1	1%
5	NH	Me	CH ₂ CH ₂ CO ₂ H	OH	274	182–414	97%	0%	-0.9	7%
6	NH	CH ₂ CH ₂ CO ₂ H	Me	OH	437	328–581	95%	0%	-1.6	1%
7	NH	Me	CH ₂ CH ₂ CONHMe	OH	41	37–46	104%	1%	-1.4	1%
8	NH	Me	CH ₂ CH ₂ CONMe ₂	OH	16	13–18	96%	1%	-1.6	1%
9	NH	Me	CH ₂ CH ₂ CH ₂ NHMe	OH	9	6–15	97%	-3%	-0.6	5%
10	NH	Me	CH ₂ CH ₂ CH ₂ NMe ₂	OH	70	59–84	94%	-5%	-1.8	1%
11	NH	Me	H	OH	76	62–93	97%	-1%	-1.2	0%
12	NH	Me	allyl	OH	24	22–27	93%	3%	-1.9	4%
13	NH	Me	n-propyl	OH	24	22–27	99%	5%	-1.6	4%
14	NH	Me	propargyl	OH	5	4–6	100%	2%	-1.1	2%
15 ^g	NH	Me	Ph	OH	0.9	0.6–1.1	105%	3%	-0.9	1%
15 ^h	NH	Me	Ph	OH	13	12–14	92%	4%	4.2	2%
16	NH	Me	Bn	OH	27	21–35	104%	3%	-0.9	3%
17	NH	Me	<i>para</i> -tol	OH	27	24–31	95%	0%	-2.0	4%
18	NH	Et	Ph	OH	5	4–6	100%	1%	-1.6	1%
19	NH	Bu	Ph	OH	6	5.6–6.0	100%	2%	-2.2	0.3%
20	NH	H	Br	H	NI ^j	NA ^k	NA	NA	NA	~100%
21	NH	Me	H	Me	NI	NA	NA	NA	NA	~100%
22	NH	Me	H	NH ₂	199	160–248	104%	5%	-1.4	2%
23	NH	Me	Ph	NH ₂	~160	107–239	100%	0%	-0.7	0%
24	S	Me	Ph	OH	35	30–41	95%	5%	-1.5	5%
25	NMe	Me	Ph	OH	34	26–46	96%	5%	-2.7	3%
Pyridine pyrazole-based scaffold					Best Fit Parameters					
cmpd		R1	R2		IC ₅₀ μM	IC ₅₀ 95% CI μM	top	bottom	Hill slope	residual
26		Me	Ph		74	62–89	95%	1%	-2.6	0%
27		Me	Bn		57	49–67	96%	-1.6%	-1.4	1%
28		Me	allyl		191	81–450	100%	2%	-0.8	2%
Pyridazine-substituted Variant					Best Fit Parameters					
cmpd		see structure above			IC ₅₀ μM	IC ₅₀ 95% CI μM	top	bottom	Hill slope	residual
29		see structure above			68	61–76	100%	3%	-1.5	1%
Carboxy-substituted Variant					Best Fit Parameters					
cmpd		see structure above			IC ₅₀ μM	IC ₅₀ 95% CI μM	top	bottom	Hill slope	residual
30		see structure above			19	15–24	107%	-2%	-0.9	0%

^aValues calculated from kinetic data using the log(inhibitor) vs. response -- Variable slope inhibition model in GraphPad Prism. ^bFitting error reported as a 95% confidence interval. ^cHighest level of enzyme activity fit as a variable in the inhibition model. ^dLowest level of enzyme activity fit as a variable in the inhibition model. ^eSteepestness, or hill slope of the dose response curve. ^fLevel of enzyme activity remaining at the highest inhibitor concentration tested. ^gValues from the FDH-based assay. ^hValues from the CTH ELISA-based assay. ⁱData reproduced from Carter *et al.* (2017): values of IC₅₀ = 12.5 μM and 800 μM when fit to a biphasic inhibition model. ^jNo inhibition seen at the highest concentration of inhibitor tested. ^kNot applicable given a lack of inhibitor efficacy.

Table S2. Crystallographic Data

	KDM4A with cmpd 26 PDB code 6G5W	KDM4A with cmpd 30 PDB code 6G5X
resolution range (Å)	46.57 - 1.826 (1.892 - 1.826)*	46.84 - 1.78 (1.843 - 1.78)
space group	P 2 ₁ 2 ₁ 2	P 2 ₁ 2 ₁ 2
unit cell a, b, c (Å), α , β , γ (°)	99.36 148.57 56.39 90 90 90	99.14 148.61 56.91 90 90 90
total np. of reflections	432868	478462
No. of unique reflections	74525 (7156)	81224 (7904)
multiplicity	5.8	5.9
completeness (%)	99.50 (97.00)	99.75 (98.15)
mean I/sigma(I)	15.78 (1.70)	21.54 (1.69)
Wilson B-factor	30.75	28.64
R-meas (%)	6.8 (100.2)	5.6 (105.3)
CC _{1/2}	99.9 (71.1)	100 (69.9)
R-work (%)	17.5 (27.9)	16.8 (27.8)
R-free (%)	21 (032.2)	20.6 (31.7)
number of non-hydrogen atoms	6250	6389
macromolecules	5723	5756
ligands	77	86
water	443	538
protein residues	692	696
RMS(bonds) (Å)	0.012	0.011
RMS(angles) (°)	1.29	1.36
Ramachandran favored (%)	98	98
Ramachandran allowed (%)	2	2
Ramachandran outliers (%)	0	0
clashscore	1.66	1.22
average B-factor (Å ²)	44.60	39.30
macromolecules	44.60	39.00
ligands	46.80	36.80
solvent	44.70	42.80

*Values in parentheses are for the respective highest resolution shell.

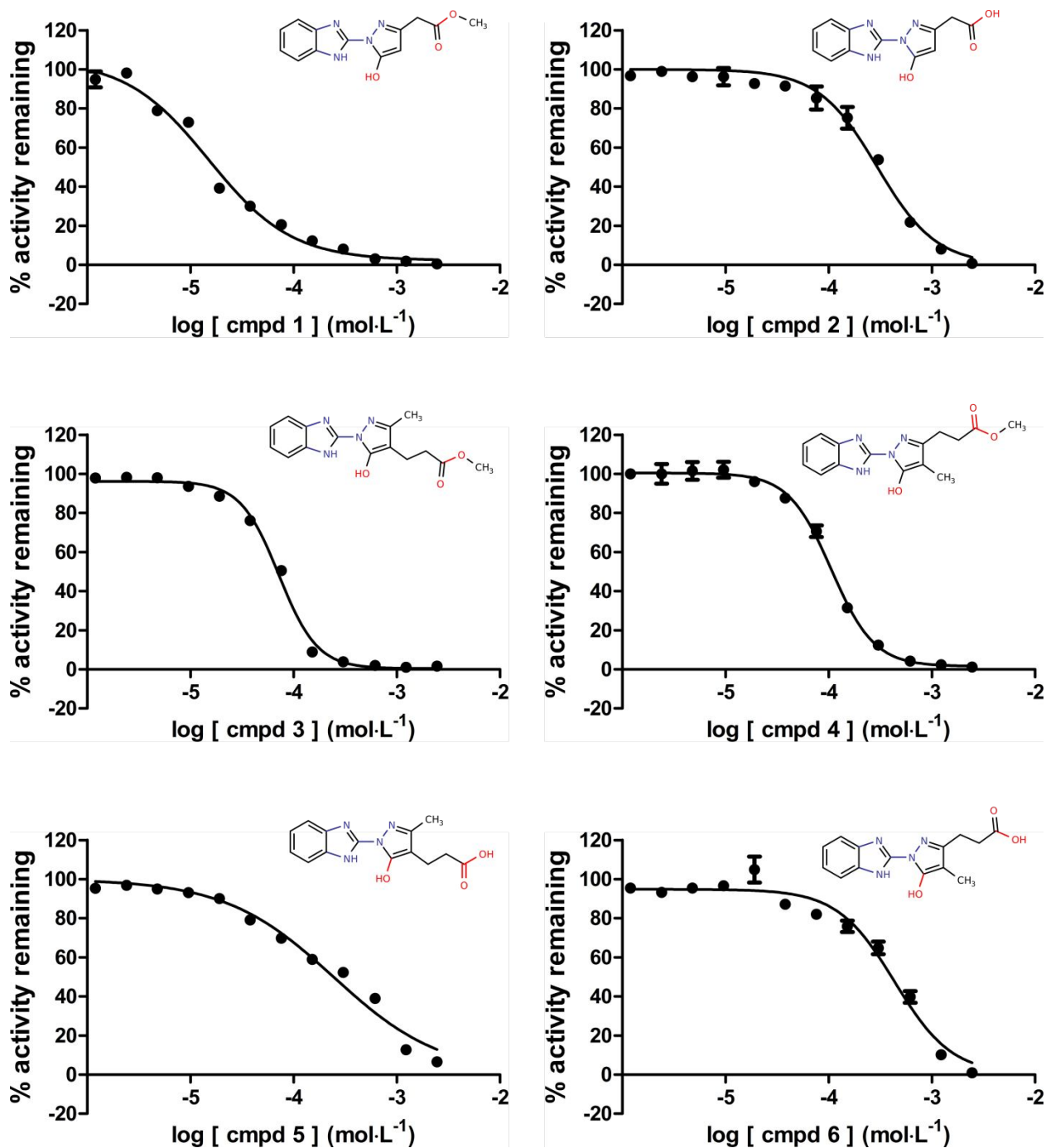


Figure S1. Inhibitory properties of selected KDM4 inhibitors, designed to assess H-bonding capacity within the KDM4E active site. Inhibition profiles resulting from FDH-based, KDM4E activity assays are depicted with best fit lines indicated using the log(inhibitor) vs. response -- Variable slope inhibition model in GraphPad Prism. The corresponding compound structures are depicted above each plot. Inhibitory profiles were assessed relative to data measured from the original HTS hit, compound **1** (top left panel).

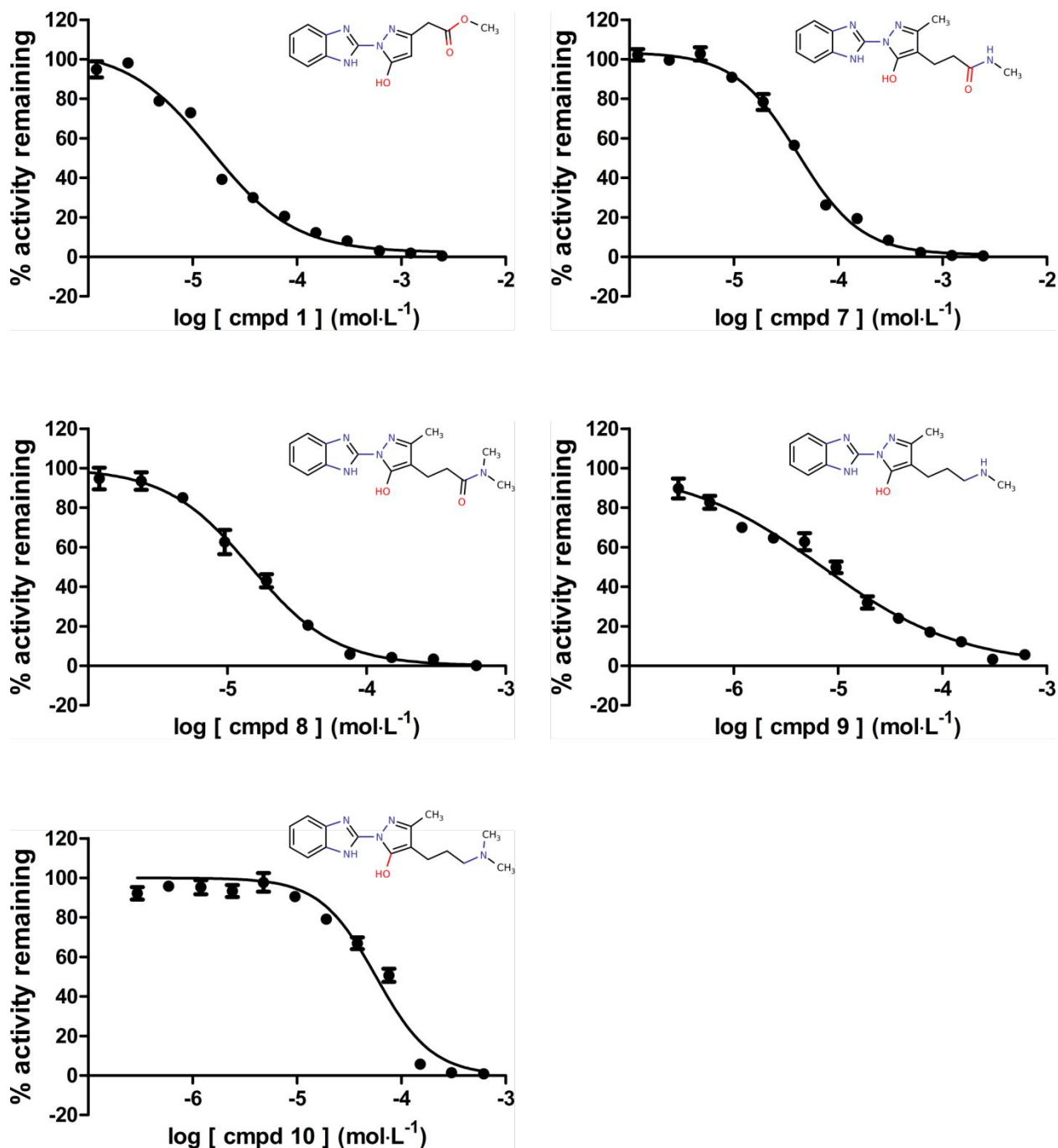


Figure S2. Inhibitory properties of selected KDM4 inhibitors, designed to assess substituted amine binding within the KDM4E active site. Inhibition profiles resulting from FDH-based, KDM4E activity assays are depicted with best fit lines indicated using the log(inhibitor) vs. response -- Variable slope inhibition model in GraphPad Prism. The corresponding compound structures are depicted above each plot. Inhibitory profiles were assessed relative to data measured from the original HTS hit, compound **1** (top left panel).

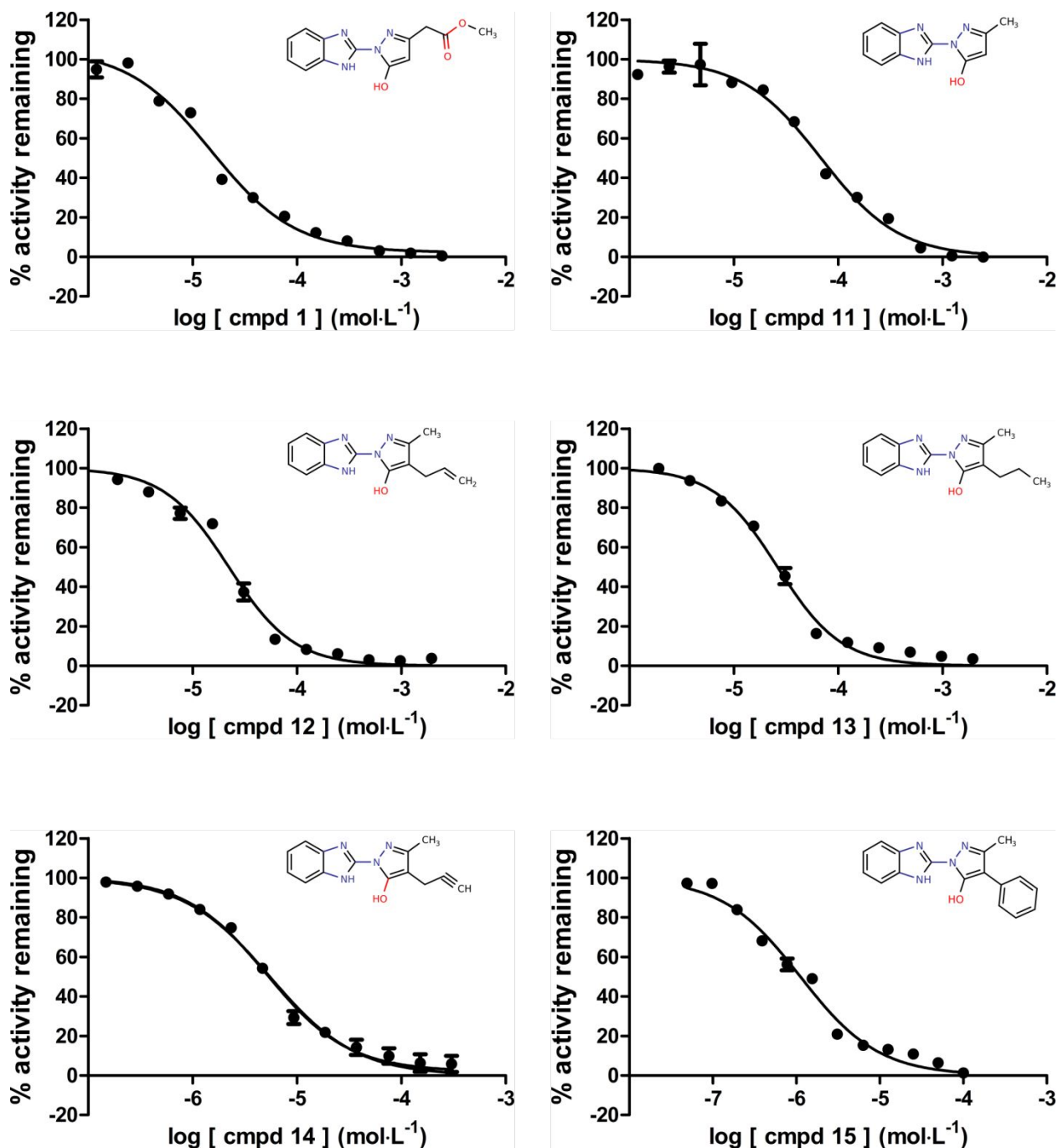


Figure S3. Inhibitory properties of selected KDM4 inhibitors, designed to assess inhibitor sidechain polarity at the R2 scaffold position. Inhibition profiles resulting from FDH-based, KDM4E activity assays are depicted with best fit lines indicated using the log(inhibitor) vs. response -- Variable slope inhibition model in GraphPad Prism. The corresponding compound structures are depicted above each plot. Inhibitory profiles were assessed relative to data measured from the original HTS hit, compound **1** (top left panel).

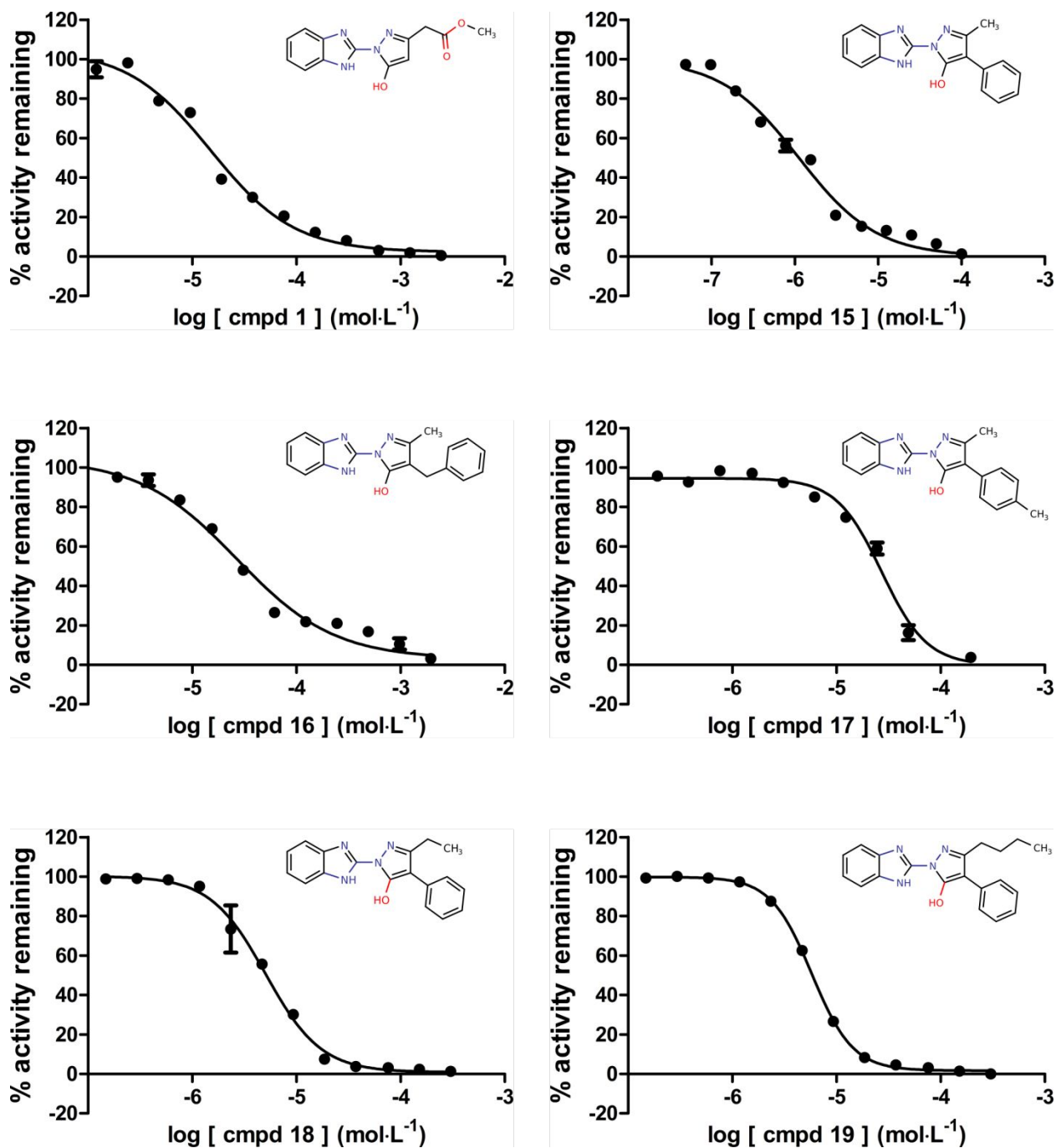


Figure S4. Inhibitory properties of selected KDM4 inhibitors, designed to further assess inhibitor sidechain polarity at R1 and R2 scaffold positions. Inhibition profiles resulting from FDH-based, KDM4E activity assays are depicted with best fit lines indicated using the log(inhibitor) vs. response -- Variable slope inhibition model in GraphPad Prism. The corresponding compound structures are depicted above each plot. Inhibitory profiles were assessed relative to data measured from the original HTS hit (compound **1**, top left) and the most potent inhibitor tested (compound **15**, top right).

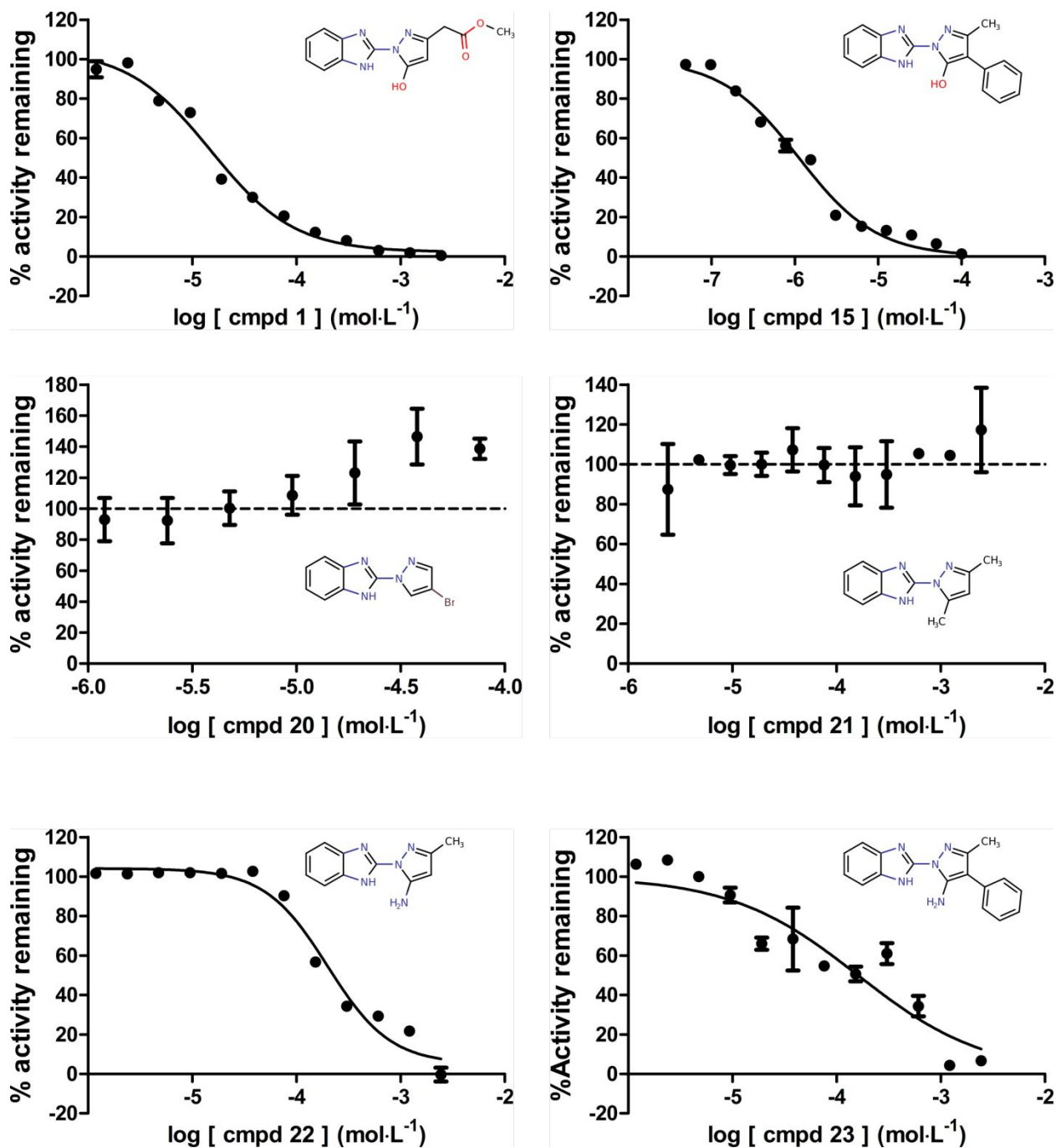


Figure S5. Inhibitory properties of focused KDM4 inhibitors, designed or selected to characterize substitutions of the pyrazole hydroxyl moiety. Inhibition profiles resulting from FDH-based, KDM4E activity assays are depicted with best fit lines indicated using the log(inhibitor) vs. response -- Variable slope inhibition model in GraphPad Prism. The corresponding compound structures are depicted within each panel. Inhibitory profiles were assessed relative to data measured from the original HTS hit (compound 1, top left) and the most potent inhibitor tested (compound 15, top right).

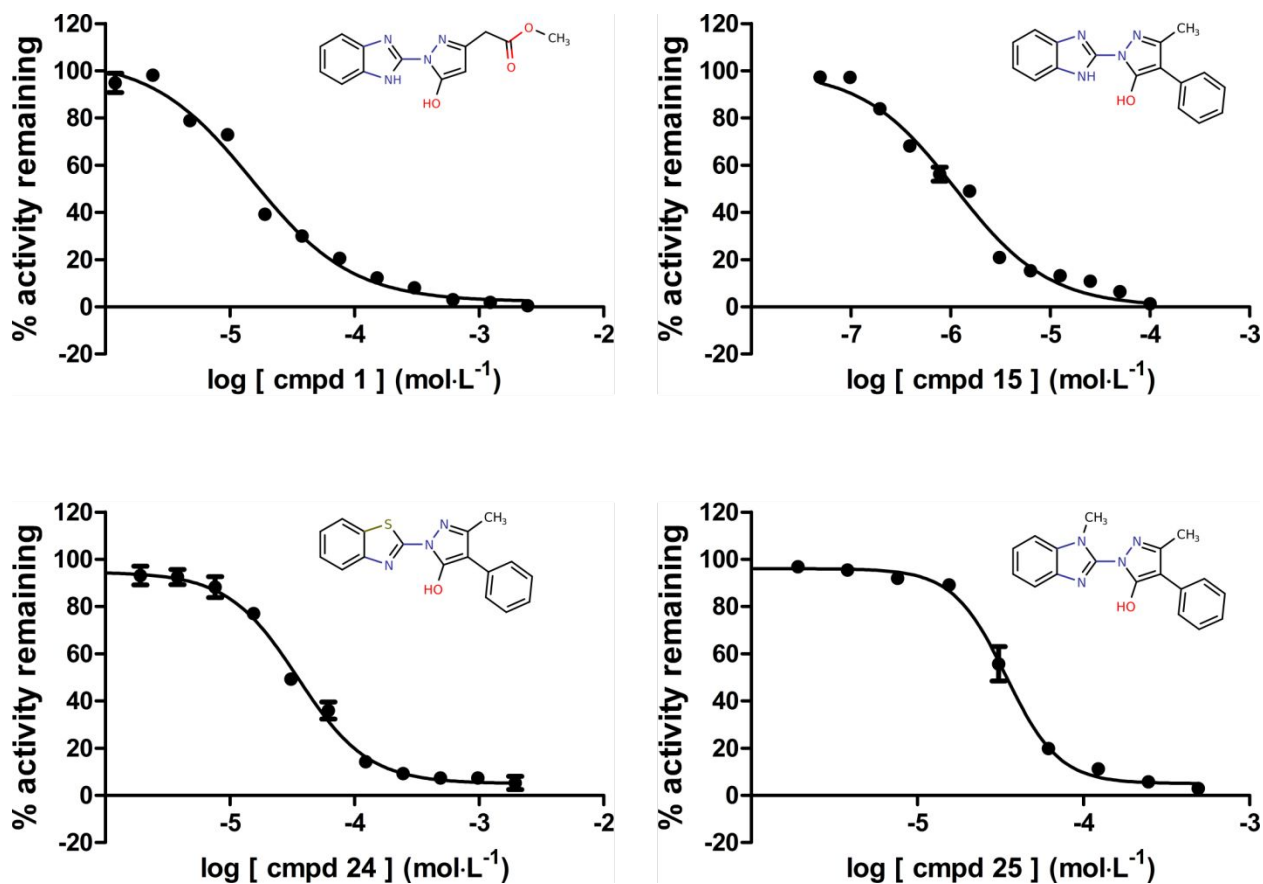


Figure S6. Inhibitory properties of selected KDM4 inhibitors, designed to assess the potential of active site Fe²⁺ chelation via the scaffold's bidentate chelation motif. Inhibition profiles resulting from FDH-based, KDM4E activity assays are depicted with best fit lines indicated using the log(inhibitor) vs. response -- Variable slope inhibition model in GraphPad Prism. The corresponding compound structures are depicted within each panel. Inhibitory profiles were assessed relative to data measured from the original HTS hit (compound **1**, top left) and the most potent inhibitor tested (compound **15**, top right).

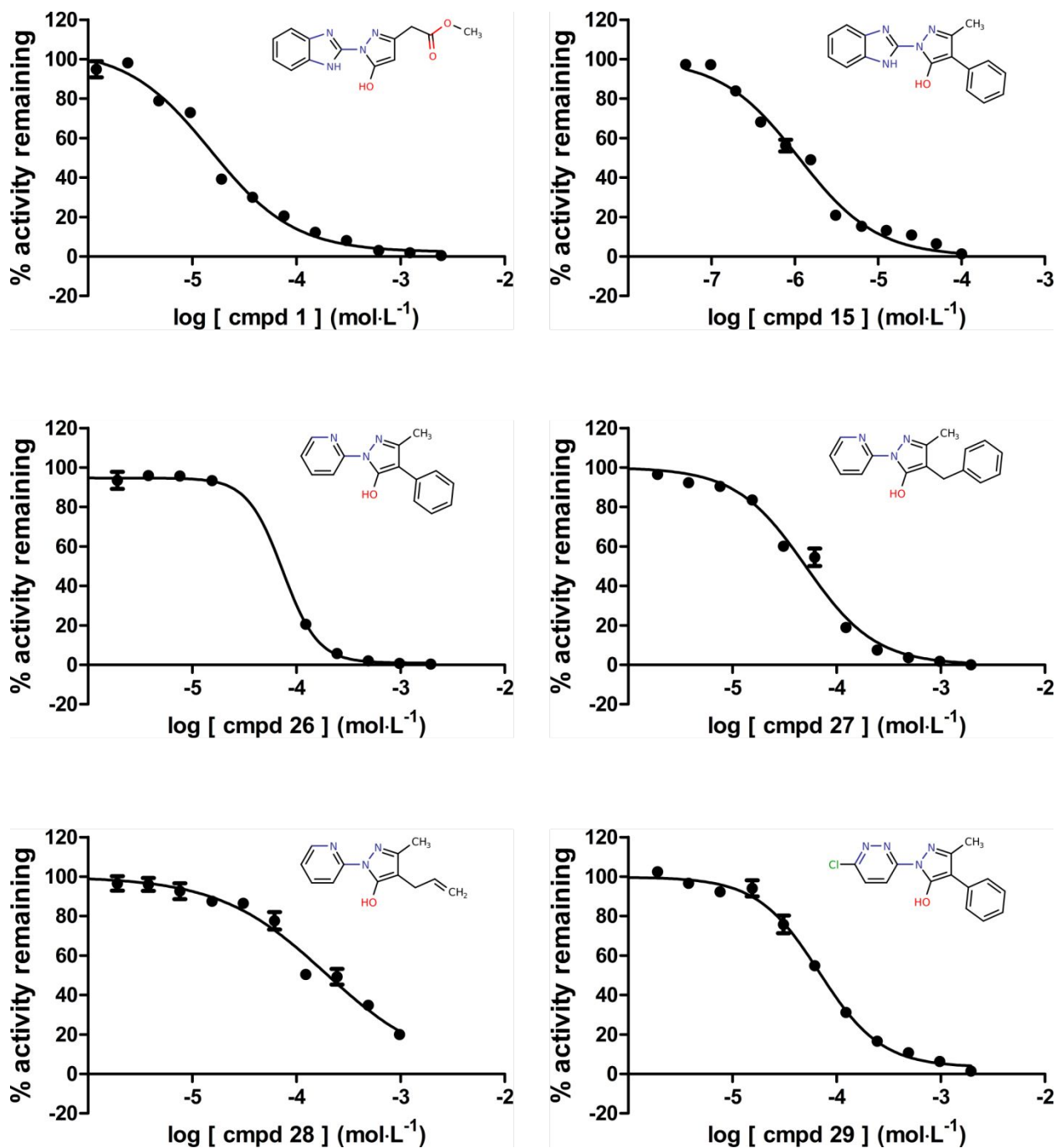


Figure S7. Inhibitory properties of selected KDM4 inhibitors, designed to assess the contribution of the scaffold's benzimidazole function towards inhibitory efficacy. Inhibition profiles resulting from FDH-based, KDM4E activity assays are depicted with best fit lines indicated using the log(inhibitor) vs. response -- Variable slope inhibition model in GraphPad Prism. The corresponding compound structures are depicted within each panel. Inhibitory profiles were assessed relative to data measured from the original HTS hit (compound **1**, top left) and the most potent inhibitor tested (compound **15**, top right).

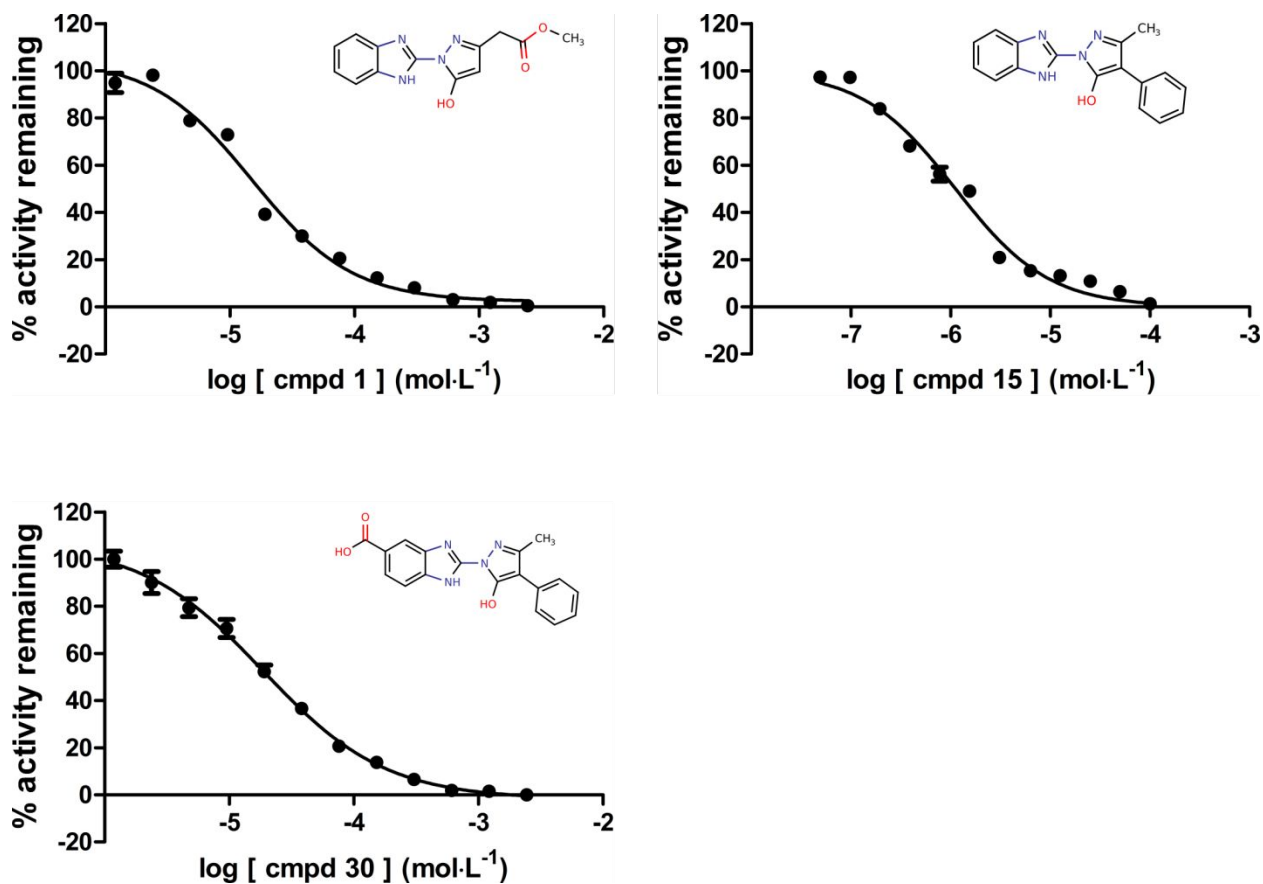


Figure S8. Inhibitory properties of selected KDM4 inhibitors, designed to assess the possibility to derivatize the scaffold's benzimidazole function. Inhibition profiles resulting from FDH-based, KDM4E activity assays are depicted with best fit lines indicated using the log(inhibitor) vs. response -- Variable slope inhibition model in GraphPad Prism. The corresponding compound structures are depicted within each panel. The inhibitory profile of **30** was assessed relative to data measured from the original HTS hit (compound **1**, top left) and the most potent inhibitor tested (compound **15**, top right).

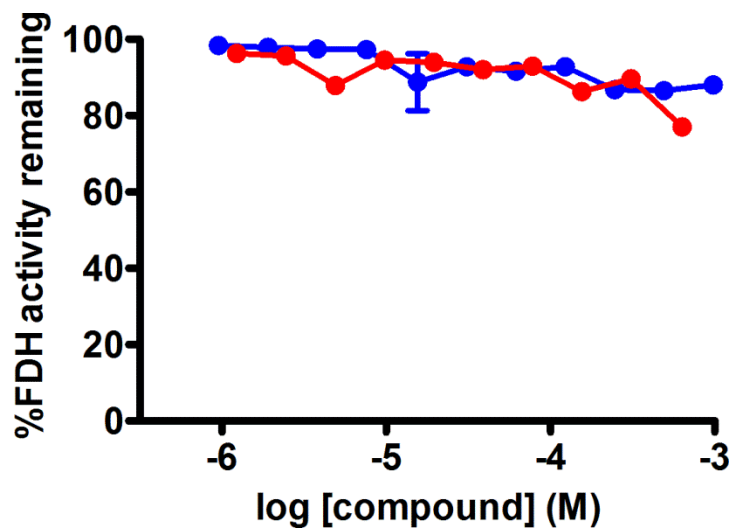


Figure S9. Enhanced properties of a benzimidazole benzylpyrazole KDM4E inhibitor do not affect activity of the coupling enzyme, formaldehyde dehydrogenase. The activity of FDH is plotted above as a function of KDM4 inhibitor concentration. Data points in blue reflect the original HTS hit (compound **1** in the main text). Data points in red reflect the most potent KDM4 inhibitor tested (compound **15** in the main text).

DU145 Cells

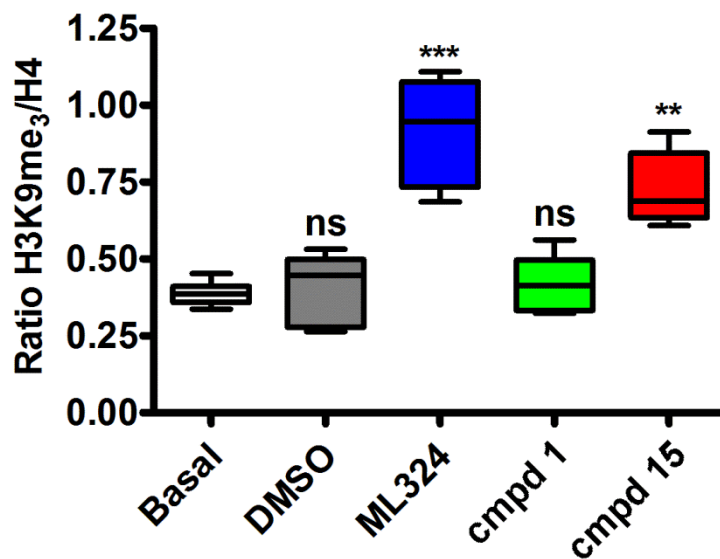


Figure S10. Compound **15** is active in cellular models of prostate cancer. Nucleosomal preparations from DU145 cells treated with membrane-permeable KDM4 inhibitors (ML324, blue; compound **15**, red) exhibit significantly higher levels of the H3K9me₃ epigenetic mark (normalized to a static histone H4 epitope), compared to untreated cells (white, labeled Basal), or to cells treated either with the non-permeable KDM4 inhibitor compound **1** (green), or with DMSO alone (grey). Statistical P values from t-tests were calculated relative to the signal arising from cells grown under basal conditions (for DMSO, ns = not significant), or relative to the signal arising from cells grown in the presence of DMSO (for ML324, ***P<0.0001; for compound **1**, ns = not significant; for compound **15**, **P=0.0016).